

Measuring Shapes of Galaxy Images II: Structure of 2MASS Galaxies

Nurur Rahman and Sergei F. Shandarin

Department of Physics and Astronomy, University of Kansas, Lawrence, KS 66045, USA;
nurur@kusmos.phsx.ukans.edu, sergei@ku.edu

ABSTRACT

We investigate a sample of 112 galaxies of various Hubble types imaged in the Two Micron All Sky Survey (2MASS) in the Near-Infra Red (NIR; 1–2 μm) J , H , and K_s bands. We use a set of non-parametric shape measures constructed from the Minkowski Functionals (MFs) for galaxy shape analysis.

Using ellipticity (E) and orientation angle (Φ), as functions of area within the isophotal contour, as shape diagnostic we have noted that the NIR elliptical galaxies with $E > 2.0$ show a trend of being centrally round and increasingly flattened towards the edge, a trend similar to images in optical wavelengths. The highly flattened elliptical galaxies show strong change in ellipticity between the center and the edge. The lenticular galaxies show morphological properties resembling either ellipticals or spirals, specially barred type. Our analysis shows that $\sim 70\%$ of spiral galaxies appear to have bar-like features while the rest are likely to be non-barred. Our results also indicate that $\sim 47\%$ of spiral galaxies have optically hidden bars.

The isophotal twist noted in the orientations of elliptical galaxies decreases with the flattening of these galaxies indicating that twist and flattening are also anti-correlated in NIR as found in optical wavelengths. The observed twists in the orientations of NIR lenticular and spiral galaxies have a wide range, varying in between $\sim 5^\circ$ to $\sim 80^\circ$.

1 INTRODUCTION

Galaxy morphology in different wave-bands provides useful information on the nature of galaxy evolution as well as about the overall distribution of galaxy constituents such as old red giants, young luminous stars, gas, dust etc. For example, the younger Population I stars associated with massive gas-rich star formation regions light up the disk galaxies in optical wavelengths. The distribution of older Population II stars, the dominant matter component near the central regions of galaxies, remains unveiled. The presence of interstellar dust hide the old stellar population especially in late-type disk galaxies. The NIR light, on the other hand, is much less affected by the interstellar dust and more sensitive to the older populations. Thus it provides a penetrating view of the core regions in disk galaxies. Therefore careful analysis of morphological differences between the optical and infrared images would not only provide valuable insight into the role of population classes in morphology but also reveal whether the discrepancies are due to singular or combined effects of extinction and population differences (Jarrett et al. 2003).

In the morphological studies of cosmological objects the most widely used technique is the ellipse-fitting method, (Carter 1978; Williams & Schwarzschild 1979; Leach 1981; Lauer 1985; Jedrzejewski 1987; Fasano & Bonoli 1989; Franx, Illingworth & Heckman 1989; Peletier et al. 1990). In this study we use a set of measures known as the Minkowski

functionals (hereafter MFs, Minkowski 1903) to analyze the morphology of NIR galaxies. Contrary to the conventional method, the MFs provide a non-parametric description of the images implying that no prior assumptions are made on the shapes of the images. The measurements based on the MFs appear to be robust and numerically efficient which had been applied to various cosmological studies e.g. galaxies, galaxy-clusters, CMB maps etc. (Mecke, Buchert & Wagner 1994; Schmalzing & Buchert 1997; Kerscher et al. 1997; Schmalzing & Gorsky 1998; Hobson, Jones & Lasenby 1999; Novikov, Feldman & Shandarin 1999; Schmalzing et al. 1999; Beisbart 2000; Kerscher et al. 2000a; Novikov, Schmalzing, & Mukhanov 2000; Beisbart, Buchert & Wagner 2001a; Beisbart, Valdarnini & Buchert 2001b; Kerscher et al. 2001b; Shandarin 2002; Shandarin et al. 2002; Sheth et al. 2003; Rahman & Shandarin 2003)

This is the second in a series of papers where we have analyzed a larger sample of 2MASS galaxies imaged at J , H , and K_s band in NIR (Jarrett 2000; Jarrett et al. 2000, Jarrett et al. 2003). We have described and tested the set of Minkowski parameters derived from the two-dimensional scalar, vector and several tensor MFs to quantify galaxy shapes for a small sample of 2MASS images in Rahman & Shandarin (2003). The measurements in Rahman & Shandarin (2003) used contour smoothing to reduce the effect of background noise. We have used the same technique in the present sample which contain NIR galaxies over the

entire range of Hubble types including ellipticals, lenticulars and spirals. The present investigation is aimed to obtain structural information of 2MASS galaxies by measuring their shapes quantified by ellipticity and orientations. As dusty regions of galaxies becomes transparent in the NIR, the imaging in this part of the spectrum would provide a clear view of the central core/bulge regions of these objects. A systematic study of NIR images would provide valuable information regarding the central structures of galaxies (e.g. optically hidden bar) which would otherwise remain absent when viewed in optical wavelengths. If only the old red giants illuminate galaxies at NIR wavelengths and are decoupled from Population I star lights, then the NIR galaxies would show weak isophotal twist in their orientations compared to those in the visual wavelengths. It would therefore be interesting to check whether the twist is wavelength dependent effect or not.

The organization of the paper is as follows: the 2MASS sample and selection criteria is given in §2, a brief discussion on shape measures is given in §3. We present the results in §4 and the conclusion are given §5. In the appendix (§6) we demonstrate the sensitivity of the Minkowski measures with illustrative examples.

2 2MASS DATA

The 2MASS catalogue present near-infrared images of nearby galaxies within red-shift range from $cz \sim 10,000$ km s⁻¹ to 30,000 km s⁻¹. The survey utilizes the NIR band windows of $J(1.11 - 1.36 \mu\text{m})$, $H(1.50 - 1.80 \mu\text{m})$ and $K_s(2.00 - 2.32 \mu\text{m})$. The 2MASS images have 1'' pixel resolution and 2'' beam resolution. The seeing FWHM values for these images are typically in between 2.5'' and 3'' in all three bands. For details of the 2MASS observation, data reduction, and analysis the readers are referred to Jarrett (2000) and Jarrett et al. (2000, 2003).

Our sample contains 112 galaxies imaged in NIR J , H , and K_s bands which includes 32 elliptical, 16 lenticulars, and 64 spirals acquired from 2MASS Extended Source Catalogue (XSC; Jarrett et al. 2003). The spiral sample contains 19 normal (SA), 21 transitional (SAB), and 24 barred (SB) galaxies. The types of all galaxies in the entire sample are followed from RC3 catalogue (de Vaucouleurs et al. 1992). The sample is statistically representative but not complete since only the bright 2MASS galaxies from three different bands are considered for the current analysis. The K_s band total magnitude for the members in the sample is within the range, $7 \leq K_s \leq 12$. The spiral galaxies with inclination up to $i \sim 60^\circ$ are included in the sample. No de-projection had been made to any of these galaxies prior to the analysis since the projection effect does not pose a serious threat to the reliability of the measurement while using parameter such as ellipticity in the structural analysis of low inclination spiral galaxies (Martin 1995; Abraham et al. 1999).

About 60% of galaxies in our sample had been studied before both in the visual and infra-red wave bands (Galletta 1980; Leach 1981; Bender & Möllenhoff 1987; Jedrzejewski 1987; Wozniak et al. 1995; Seigar & James 1998). The motivation behind constructing our sample is to make a comparative analysis with previous results and to investigate the

galaxies with new tools to gain further insight about the overall morphology of galaxies in infra-red wave-bands.

We use the 2MASS ellipticity and orientation measured from K_s band $3 - \sigma_n$ isophote as a reference. All galaxies in our sample are flat fielded and background subtracted. Except three ellipticals, the rest of the galaxies are foreground and background star removed. These galaxies where foreground star is embedded into images are included purposely to illustrate the sensitivity of the Minkowski morphological measures as explained in the appendix.

3 MINKOWSKI FUNCTIONALS AS SHAPE DESCRIPTORS

The full morphological description of structures requires both topological and geometrical characteristics. The MFs consist of a set of measures carrying both geometric (e.g. areas, perimeters) and topological (the Euler characteristic) information about an object. The functionals obey a set of covariance properties such as motion invariance, additivity and continuity (see e.g. Schmalzing 1999; Beisbart 2000). For this investigation we use two-dimensional scalar, vector and a selection of tensor MFs as described in Rahman & Shandarin (2003).

We treat every image as a set of contour lines built from a pixelized map. Every contour is constructed by linear interpolation at chosen surface brightness levels. The measurements provide three scalars, three vectors (centroids) and a total nine components of three symmetric tensor functionals for every contour (see appendix for more). After obtaining the eigen values of the tensors, the axes and orientations of “auxiliary ellipses” are constructed. The construction of an “auxiliary ellipse” is as follows: suppose we have the eigen values of the area tensor. We then ask what possible ellipse one might construct whose inertia tensor would give exactly the same eigen values as the area tensor. When that particular ellipse is found, we call it the “auxiliary ellipse” corresponding to the area tensor. The auxiliary ellipses corresponding to the perimeter and EC tensors are constructed in a similar manner.

To discern morphologically different objects, therefore, we use the parameters (ellipticity and orientation) of the auxiliary ellipses rather than the eigen values of the tensors themselves. The use of these ellipses effectively relates the contour to an ellipse: the similarity of three auxiliary ellipses is a strong evidence that the shape of the contour is elliptic. For example, in case of a perfect elliptic contour, the auxiliary ellipses would be the same. In particular, the areas of all auxiliary ellipses would be equal to the area of the contour (A_{cont}) as well as the perimeters of the auxiliary ellipses would be equal to the perimeter of the contour (P_{cont}). In addition, the orientations of all three auxiliary ellipses would coincide with orientation of the contour. Therefore all three auxiliary ellipses would be on top of each other overlapping with the contour. The vector centroids will coincide for a perfect elliptic contour. But this does not guarantee whether the contour itself is elliptic in nature since for any contour having a point symmetry the centroids will coincide. However for a non-elliptic contour all three auxiliary ellipses would be different (see Fig. 1 Rahman & Shandarin 2003).

In order to reduce the effect of noise on the image we

have used a simple smoothing technique. Instead of smoothing the whole image, we smooth contours at each brightness level using a procedure known as the un-equally weighted moving average method. The goal of this smoothing is to restore the initial unperturbed contour as much as possible and measure its morphological properties. The implementation of smoothing is described in detail in Rahman & Shandarin (2003). The contour smoothing makes considerable improvement of all the estimates of ellipticity constructed from tensor functionals (see e.g. Figs 8 and 9 in Rahman & Shandarin, 2003). In this investigation, therefore, we have focused on the results obtained from smoothed contours. We would like to mention here that as a result of smoothing occasionally contour crossing occurs at the outer regions of galaxies where smoothed outer contour cross the inner one. This effect is due to the nature (linear) of the smoothing. In all cases the area within the contours remains unaffected and thus do not affect the results.

4 RESULTS

We use ellipticity (E) and orientation (Φ) as shape characteristics. These two parameters are well known and had been applied to quantify properties of elliptical galaxies (e.g. Carter 1978; Williams & Schwarzschild 1979; Leach 1981, Lauer 1985; Jedrzejewski 1987; Fasano & Bonoli 1989; Franx, Illingworth & Heckman 1989; Peletier et al. 1990). In many recent works this set of parameters have been used to obtain information on different structural components e.g. bar, bulge, disk etc. of disk galaxies (Athanasoula et al. 1990; Martin 1995; Wozniak et al. 1995; Rozas, Knapen & Beckman 1998; Abraham & Merrifield 2000; Laurikainen, Salo & Rautainen 2002; Peng et al. 2002).

We measure E and Φ for a set of contours obtained at different surface brightness levels. Generally these two parameters vary with the area of the contour i. e. $E = E(A)$ and $\Phi = \Phi(A)$. Galaxies with different morphologies appear to show characteristic signatures in the E profile. For example, profile of elliptical galaxies is generally monotonic but for the barred galaxies it shows distinct peak with a relatively round central region (i. e. signaling the presence of central bulge). On the other hand for a multi-barrred system, several peaks appear on the profile. Note that the E parameter alone can be used to isolate galaxies at least into two broad bins: non-barrred and barrred systems. For finer distinction we need to use other parameters such as luminosity, color, surface brightness, half light radius etc.

Elliptical galaxies usually show twists (i.e. change in the orientation of auxiliary ellipse) in the Φ profiles with varied strength depending on the flattening of the contours. Disk Galaxies, on the other hand, not only have very large twist in their orientations but also have characteristic features such as a sharp kink or two different but approximately constant orientations with an abrupt change in between.

We analyze each galaxy at 30 different brightness levels where the levels correspond to equally spaced area in logarithmic scale covering almost the entire region of each galaxy. At every brightness level contours are constructed and subsequently smoothed. The area, perimeter and EC auxiliary ellipses are measured for smooth contours. We present our final results as in the Fig. 1 to Fig. 14 using

the parameters only from the area tensor auxiliary ellipse. We provide illustrative examples in the appendix for making this choice. For each galaxy we show the E and Φ of the auxiliary ellipse as a function of scalar area (A_S) where A_S is the total area enclosed by the contour.

A thick dashed line is used to show the mean values of E and Φ calculated from J, H , and K_s bands. Two thin solid lines are used to show the maximum and minimum of the measures obtained from these bands. The difference between these two thin lines is used to quantify the scatters (δE and $\delta \Phi$) in ellipticity and orientation. We use the scatter as the indicator to measure the dependence of galaxy shapes on different colors. For every sample of galaxies the result is presented in increasing order of E where the 2MASS ellipticity is used to sort the galaxies.

Ellipticals

The sample of elliptical galaxies has been divided into two groups. Group 1 contains galaxies with small ellipticities ($E \leq 2.0$) while group 2 have galaxies with $E > 2.0$. For the orientations of galaxies we followed the convention where North is up and East is on the left. The properties of elliptical galaxies in two group are briefly discussed below.

Group 1:

Ellipticity: The E profiles of galaxies in this group are shown in Fig. 1. Galaxies such as NGC 4374 and NGC 4261, as shown in Fig. 1 with a mark ‘‘A’’, have uncommon E profiles compared to other galaxies in this group. The galaxies are more elongated in the middle region, $1.8 < \log_{10} A_S < 3.0$, than either around the center or near the edge. The overall change in ellipticity shown by these galaxies is $\Delta E \sim 1.0$ and their E profiles look like ‘‘centrally arched’’. This particular type of behavior is shown only by round ellipticals and is absent in elongated galaxies. The optical morphology of NGC 4374 and NGC 4261 had been analyzed by Bender & Möllenhoff (1987) in V, R , and I bands. In comparison to their results, we note that NGC 4374 shows slightly higher ellipticity ($\Delta E \sim 0.5$) in NIR; NGC 4261 has higher ellipticity ($\Delta E \sim 0.75$) in optics but has similar E profile in both wavelengths.

The following three galaxies are shown with a ‘‘S’’ mark in Fig. 1: NGC 4278, NGC 3193, and NGC 3379. These galaxies have sharp kinks in the E profiles with an overall change $\Delta E \sim 1.0, \sim 1.5$, and ~ 0.5 respectively. These sharp changes in ellipticity are contributed by the foreground star and do not corresponds to any structural feature (see appendix).

Among other ellipticals in this group NGC 4458, NGC 2986, NGC 4494, NGC 3158, VCC 1737, and NGC 3159 have pretty much stable E profile ($\Delta E \sim 0.5$) compared to NGC 4955, NGC 3226, NGC 3962, NGC 2778, and NGC 6146, where these four galaxies have higher variation in their profiles ($\Delta E \sim 1.5$), specially near the center. The galaxies in this group 1 show very small scatter, $\delta E \sim 0.1 - 0.5$. For most of these galaxies our estimate of ellipticity, at least near the edge, is in nice agreement with 2MASS.

Orientation: The orientations of galaxies are presented in Fig. 2. We start with the galaxies having ‘‘central arch’’ in their shape profiles i. e. NGC 4374, NGC 4261. The average twist measured in their orientations is $\Delta \Phi < 10^\circ$ with a scatter on average $\delta \Phi \sim 4^\circ$ which increases towards the central region. For both NGC 4374 and NGC 4261 our

estimates are close to the results obtained in the analysis in optical wavelengths (Bender & Mollenhoff, 1987). For NGC 4374 our measurement of Φ differs $\sim 8^\circ$ from 2MASS and for NGC 4261 the two measurements are within $\sim 3^\circ$ except for a very short region at the edge where they disagree by $\sim 8^\circ$. For NGC 4458 the twist near the edge is $\Delta\Phi \sim 30^\circ$. It is pretty much stable from the center up to $\log_{10} A_S \approx 2.8$. It is also one of the few galaxies in this group with relatively large scatter.

Among the galaxies that have foreground star embedded into images, only NGC 3193 shows a notable kink in its orientation with $\Delta\Phi \sim 26^\circ$. The dip in the Φ profile of NGC 4278 makes the twist $\Delta\Phi \sim 20^\circ$ around the region of the galaxy where the foreground star is embedded. NGC 3379 does not show any unusual feature like an abrupt change in its Φ profile; instead its position angle as well the scatter gradually increases towards the galactic center with an overall twist of $\Delta\Phi \sim 20^\circ$. Both NGC 4278 and NGC 3193 have less scatter compared to NGC 3379 at all distance from galactic center. Note that the presence of a star on the galaxy contours may or may not be detected via Φ profile. The E profile, on the other hand, is capable to signal any type of noise on the contour. The reason why the presence of a star on the contours may be missed as a signature on the Φ profile is that if the lobe on the contour attributed by the star happen to be along the major axis, which is the case for NGC 3379, it remains unnoticed and no kink appears in the Φ profile. On the other hand if the lobe is slightly off the major axis, it change the orientation of the contour significantly with respect to the inner or outer contours unaffected by the star. This is the case for NGC 4278 and NGC 3193.

In spite of being a round galaxy (E1+), NGC 4494 has remarkably low twist ($\Delta\Phi \sim 2^\circ$) and scatter ($\delta\phi \sim 5^\circ$) in its orientation. The twists noted in NGC 3158, NGC 4955, NGC 2778 and NGC 6146 are $\sim 30^\circ$, $\sim 10^\circ$, $\sim 20^\circ$ and $\sim 10^\circ$ respectively. The scatter among these galaxies varies in the range $\delta\phi \sim 5 - 20^\circ$.

Our estimate for NGC 2986, VCC 1737, NGC 3159, and NGC 3226 coincide with the 2MASS at least near the edge but at the center the disagreement is quite large: NGC 2986 ($\sim 12^\circ$), VCC 1737 ($\sim 30^\circ$), NGC 3159 ($\sim 30^\circ$), NGC 3226 ($\sim 20^\circ$). Among these galaxies VCC 1737, NGC 3159, and NGC 3226 have orientations quite similar to disk galaxies as shown later in this section. The Φ profiles of VCC 1737 and NGC 3226 appear “arch like” where NGC 3226 has a longer arch compared VCC 1737. These four galaxies also have larger scatter in their orientations.

Group 2:

Ellipticity: The E profiles of galaxies in group 2 are shown in Fig. 3. The elliptical galaxies with $E > 2.0$ show a “centrally round” trend in their profiles. The variation in E becomes stronger with the increasing flattening of galaxies. The overall change in E observed from the center to the edge varies from galaxy to galaxy: from as low as ~ 2.0 (NGC 315) to as high as ~ 4.0 (NGC 3377).

Except a few galaxies the shape measurement nicely coincides in all three bands. The K_s band measurement of NGC 2778, NGC 3226, NGC 4494, and NGC 5582 show slightly lower ellipticity (≤ 0.2) around $2.0 \leq \log_{10} A_S$ compared to other two bands. Most of our estimates are in agreement at the edges with the 2MASS except for NGC 1052, NGC 4125, NGC 3377, and NGC 4239 as shown in Fig.

3. For the first three among these galaxies, our results are higher compared to 2MASS where $\Delta E \sim 1.0$. For NGC 4239 our calculation shows lower E at all distance from galactic center and the disagreement amounts to $\Delta E \sim 1.0$.

Note that the discrepancy between our estimate and the 2MASS arises mostly for the flattened galaxies, specially towards the center. The E profiles of these galaxies have similar scatters to those in group 1.

Orientation: The orientations of galaxies in this group are presented in Fig. 4. The ellipticals have quite stable orientations with relatively low twist and scatter compared to those in group 1. The $\Delta\Phi$ is within 10° with $\delta\Phi \sim 2 - 10^\circ$ for most of these galaxies beyond $\log_{10} A_S \geq 1.5$. For NGC 315, NGC 3091, and NGC 5582 the twist increases up to $\sim 15^\circ$. The scatter for several galaxies increases up to $\sim 20^\circ$ in the region $1.5 \leq \log_{10} A_S$.

Our estimate of orientations for all these galaxies in group 2 are within 10° of 2MASS measurements. The agreement is better compared to the measurements in group 1. The relatively small twist noticed for ellipticals with $E > 2.0$ suggest that flattening and isophotal twist are most likely anti-correlated in the NIR wave-bands. This results is in agreement with the (optical) correlation found by Galletta (1980) who noted that the maximum apparent flattening and the highest observed twist are inversely related.

Lenticulars

The sample of lenticulars contains 16 galaxies. The ellipticity and orientation of these galaxies are shown in Figs 5 and 6 respectively.

Ellipticity: For NGC 1315 our estimate shows slightly round ($E \sim 0.5$) inner part compared to 2MASS ($E \approx 0.9$) in between $1.2 \leq \log_{10} A_S \leq 2.6$ suggesting large spherical bulge for the galaxy. Within a small region ($2.6 \leq \log_{10} A_S \leq 3.6$) the galaxy shows a sudden large variation in its shape ($\Delta E \sim 2.5$). The two other galaxies, i. e. NGC 5228 and NGC 4659, have similar behavior.

The ellipticity variation in NGC 1400 profile is quite small ($\Delta E < 0.3$). Its profile is very stable beyond $\log_{10} A_S \geq 1.7$. For this galaxy our estimate ($E \sim 1.2$) gives more round shape compared to 2MASS ($E \sim 2.0$). In this group, NGC 3665 is the only galaxy that have the least variation in its E profile. It has a remarkably stable shape at all distance from the galactic center. NGC 3111 is another galaxy which appears more round at all distance from the galaxy center according to our estimate as compared to 2MASS and the disagreement between the measurements is in between $\sim 0.6 - 1.5$. The following galaxies have pretty much similar E profiles : NGC 3598, IC 4064, NGC 3816, NGC 3768, and NGC 2577. These galaxies appear to be more elongated at the edge compared to the central region, a behavior is similar to the elliptical galaxies.

The E profiles of the following five galaxies show bar-like feature: NGC 4620, NGC 3805, IC 3065, NGC 2544, and NGC 4014. These galaxies are labeled as “IB” in their corresponding panels where “IB” stands for infra red bar. Note that we call a profile bar-like if it shows peak(s) as result of rise and fall in ellipticity. The lenticular galaxies have relatively large scatter compared to ellipticals and the E profiles of these galaxies are similar to that of ellipticals. As mentioned above some of these galaxies also show bar-like features. For most of these galaxies the ellipticity in the

central region shows quite large disagreement with 2MASS. But near the edge, both measurements are in good agreement for almost all galaxies.

Orientation: The twist and the scatter measured in the orientation of lenticular galaxies are larger than elliptical galaxies. The twist for NGC 1315 and NGC 5228 is $\sim 25^\circ$ and $\sim 15^\circ$ respectively. The overall twist for NGC 4659 is quite large, $\Delta\Phi \sim 60^\circ$; the orientation of this galaxy experiences a large change within $1.5 \leq \log_{10} A_S \leq 2.3$.

The twists estimated for NGC 1400, NGC 3665, and NGC 3111 are $\sim 10^\circ$, $\sim 5^\circ$, and $\sim 10^\circ$ respectively where NGC 1400 and NGC 3111 have larger scatters compared to NGC 3665. The orientations of NGC 3598 and IC 4064 have almost equal amount of twist, $\Delta\Phi \sim 20^\circ$. They also have equal amount of scatter in their orientations. For NGC 3816 we note $\Delta\Phi < 10^\circ$ with $\delta\phi \sim 5^\circ$. Our measurement indicates the central region of NGC 3768 is more inclined compared to the outer part and shows an overall $\Delta\Phi \sim 15^\circ$, a trend similar to NGC 4659. The orientation of NGC 2577 has $\Delta\Phi \sim 5^\circ$ with small scatter for $\log_{10} A_S > 1.7$.

Among “IB” galaxies, NGC 4620 and IC 3065 have very large twists compared to other three galaxies. They have $\Delta\Phi \sim 50^\circ$ and $\sim 30^\circ$ respectively. For NGC 3805 and NGC 2544 the orientations change gradually inwards with $\Delta\Phi \sim 20^\circ$ and $\sim 30^\circ$ respectively; NGC 4014 has the least twist ($\Delta\Phi < 4^\circ$) and scatter ($\delta\phi \sim 2^\circ$) among these galaxies.

Lenticular galaxies with ellipticity $E > 3.0$ are observed to have less scatter compared to their round counterparts. The scatter in round lenticulars are large and varies at different regions from galaxy centers.

Spirals

The sample of spirals has been divided into four groups based on the degree of scatter (δE) observed in the E profiles measured in three different bands. Group 1 contains spirals that have the least scatter while group 4 has galaxies with the largest scatter. Galaxies with $\delta E \leq 0.5$ are included into group 1, for group 2 the range is $0.5 < \delta E \leq 1.$, those with $1.0 < \delta E \leq 2.0$ are in group 3 and finally galaxies with $\delta E > 2.0$ are taken into group 4. The grouping of the spiral sample has been done by visual examination and therefore it is quite crude. The motivation is to highlight the interesting features appeared in the shape profiles of spiral galaxies in NIR. In each of these groups, the galaxies have been ordered by increasing ellipticity. A brief discussion of the properties of each group members are given below.

Group 1:

Ellipticity: The E profiles of the galaxies in this group are shown in Fig. 7. Only four galaxies are optically classified (RC3) as barred systems. These are NGC 4262, NGC 4024, NGC 3384, and NGC 4394. The distinctive feature of their shapes i.e. clear appearance of peak(s) in their shape profiles, indicates (qualitatively) similar morphology both in optical and NIR. The central region ($\log_{10} A_S \leq 2.1$) of NGC 4262 is highly round ($E < 0.5$). This suggests a large central bulge most likely spherical in nature. The least scatter (δE) in the profile of NGC 3384 compared to other galaxies gives it a unique feature. This galaxy has a very short ($2.6 \leq \log A_S \leq 3.2$) but highly round ($E < 0.5$) region separating the central part from the edge.

In this group, optically classified non-barred systems showing feature similar to barred galaxies are IC 3927, NGC

3177, NGC 3684, NGC 3912, and UGC 5739. These galaxies are labeled as “IB” as shown in Fig. 7 where “IB” stands for infra red bar. Among these five galaxies, NGC 3177 and NGC 3684 are likely to have two distinct bars. According to RC3 classification both of galaxies are early type normal spiral but their NIR morphology appear to be complex. Our analysis shows that both secondary (inner) and primary (outer) bar of NGC 3177 has similar flattening ($E \sim 2.0$). For NGC 3684 the secondary bar is stronger ($E \sim 4.5$) than the primary ($E \sim 2.0$). Out of these five galaxies only two are SA spirals: NGC 3177 SA(rs)b and NGC 3684 SA(rs)bc.

NGC 4151 is the most round galaxy among the members of this group. It has $E < 0.5$ from the galactic center up to $\log_{10} A_S \approx 3.2$, beyond this limit the ellipticity increases a little bit. This galaxy, an intermediate ringed transitional spiral, is likely to be dominated by a very large spherical bulge. The profiles of IC 3831, NGC 4143, NGC 3418, and NGC 5326 are quite similar to elliptical galaxies. These galaxies are likely to have large and slightly flattened bulges with elongation, $E \approx 2.0$.

The ellipticity of NGC 4651 increases from the center reaching a short plateau in between $2.0 \leq \log_{10} A_S \leq 2.5$. Then in between $2.5 \leq \log_{10} A_S \leq 3.2$ it gives a narrow peak in the profile. The galaxy maintain a constant ellipticity afterwards up to the edge. A similar kind of behavior is noticed in the profile of NGC 3815. Its ellipticity increases from the center, reach a plateau in the region $2.6 \leq \log_{10} A_S \leq 3.0$, and increases again.

Except NGC 3684, NGC 4651, and NGC 5739, the remaining 13 galaxies in this group are early types spirals. NGC 3684 and NGC 4651 are, respectively, intermediate and late-type normal spiral whereas NGC 5739 is irregular Magellanic type. Apart from NGC 4151 and UGC 5739, our estimate for all other galaxies in this group is in quite good agreement with 2MASS. For NGC 4151 a large disagreement ($\Delta E \sim 2.0$) with 2MASS is noted while for UGC 5739 the deviation is slightly smaller ($\Delta E \sim 1.5$).

Orientation: The orientations of galaxies in this group are presented in Fig. 8. The overall twists ($\Delta\Phi$) in these galaxies are in range of $\sim 5^\circ - 50^\circ$. Apart from NGC 4262 and NGC 4151, the observed scatter ($\delta\Phi$) is small for all other galaxies. The optical barred galaxies i.e. NGC 4262, NGC 4024, NGC 3384, NGC 4394 have $\Delta\Phi \sim 50^\circ$, $\sim 15^\circ$, $\sim 20^\circ$, and $\sim 30^\circ$ respectively. The orientation of the barred galaxy NGC 4262 is constant along the region of the bar ($2.0 \leq \log_{10} A_S \leq 3.0$), however, the directions at the central bulge and the outer disk regions are different. The barred galaxy NGC 3384 has a narrow and sharp peak in the region $2.5 \leq \log_{10} A_S \leq 3.1$ in its Φ profile. Its orientation stays at the same angle before and after the peak.

Systems optically classified as non-barred but having bar-like features in the NIR ellipticity profiles (“IB”) show a wide range in isophotal twists. Here we mention the individual $\Delta\Phi$'s: IC 3927 : $\sim 25^\circ$, NGC 3177 : $\sim 50^\circ$, NGC 3684 : $\sim 20^\circ$, NGC 3912 : $\sim 8^\circ$, and UGC 5739 : $\sim 5^\circ$. The profiles of NGC 3177 and NGC 3684 have constant orientations from the galactic center up to $\log_{10} A_S \approx 1.8$. The orientations change in the region $1.8 \leq \log_{10} A_S \leq 2.9$ and produce a bump-like feature. The orientations go down slightly after the bumps. Later they start going up and become constant beyond $\log_{10} A_S \approx 3.2$. The two highly flattened galaxies, NGC 3912 and UGC 5739, have remarkably small isophotal

twist in spite of the bar-like features apparent in their shape profiles. These two galaxies clearly show that disk galaxies which appear to have bar-features in the NIR ellipticity profiles not necessarily have a large change in their orientations.

NGC 4151, the most round galaxy in this group, shows the largest scatter in its orientation. Since highly round contours can be perturbed easily by noise, it is not surprising that the galaxy would have large difference in its orientation at different wave-bands since these bands have different Signal-to-Noise (S/N) ratios. The galaxy shows a twist of $\Delta\Phi \sim 20^\circ$. The profile of NGC 4651 has a large dip in the region $2.0 \leq \log_{10} A_S \leq 3.4$. Both IC 3831 and NGC 5326 experience similar deviation in their orientations with $\Delta\Phi \sim 10^\circ$. The overall twist in NGC 4143 is $\Delta\Phi \sim 20^\circ$. Its profile is quite similar to the barred galaxy NGC 3384 although the change in orientation is much more smooth compared to the abrupt change in NGC 3384. For NGC 3418 the observed twist is $\Delta\Phi \sim 15^\circ$ while for NGC 3815 it is $\Delta\Phi \sim 20^\circ$.

Group 2:

Ellipticity: The E profiles of galaxies in this group are shown in Fig. 9. It contains seven galaxies that are optically classified as barred systems: NGC 3974, IC 357, NGC 4662, NGC 6347, NGC 5737, UGC 2585, and IC 568. The NIR ellipticity profiles of these galaxies indicate structures similar to optical. Among these galaxies only NGC 6347 has the characteristic signature to be considered as a double-barred system with a primary bar ($E \sim 5.0$) slightly stronger than the secondary ($E \sim 4.5$).

The following four galaxies are optically classified non-barred spirals: NGC 4146, NGC 4152, IC 863, and UGC 5903. These galaxies show bar-like features in the NIR ellipticity profiles (“IB”). The first three galaxies are likely to double-barred systems as their profiles show two different peaks at two different regions of galaxies. In NGC 4146, the bars are of different strengths; the inner secondary bar ($E \sim 4.0$) being stronger than the outer primary ($E \sim 2.0$). In NGC 4152 and IC 863, both bars have equal strength ($E \sim 3.0$).

In the E profiles of the following galaxies, NGC 3277, NGC 3667, NGC 4714, and NGC 5478, the ellipticity grows from the galactic center towards the edge without any significant feature. The projected shapes of NGC 3277 and NGC 4714 are quite similar to elliptical galaxies whereas NGC 3667 and NGC 5478 show dips in their profiles unlikely for any early-type galaxies. These spirals are likely to contain two principle components: inner bulge and outer elongated disk. The overall shape of NGC 3277 is very round compared to other three galaxies. The profile of NGC 4193 is different as compared to other galaxies in this group. After rising sharply and reaching a peak, it has two small but distinct dips. This galaxy is a late-type transitional spiral and is likely to have a round bulge with a highly flattened disk. Its shape is also quite similar to NGC 4651 which is a galaxy in spiral group 1.

Orientation: The orientations of the galaxies in this group are shown in Fig. 10. The overall twists ranges in between $\sim 10 - 60^\circ$. For optical barred galaxies the overall twists that we have estimated are NGC 3974 : $\sim 40^\circ$, IC 357 : $\sim 60^\circ$, NGC 4662 : $\sim 30^\circ$, NGC 6347 : $\sim 20^\circ$, NGC 5737 : $\sim 20^\circ$, UGC 2585 : $\sim 20^\circ$, and IC 568 : $\sim 30^\circ$. The Φ profiles of NGC 3974 and IC 357 have similar characteristics: a con-

stant direction along the central bars while the orientation changes in the central bulge and outside disk. For both NGC 4662 and NGC 5737, the disk is more inclined compared to the central bar.

Among the NIR spirals with bar-like features (“IB”), NGC 4146 has the largest twist, $\Delta\Phi \sim 60^\circ$. The twists noted in other “IB” galaxies are, NGC 4152: $\sim 40^\circ$, IC 863: $\sim 30^\circ$, and UGC 5903: $\sim 20^\circ$. The orientation of NGC 4152 shows two kinks where the inside kink is stronger than the outer one. For “IB” double barred system IC 863, the orientation takes two different constant directions along two different bars. The sudden change in its direction from the secondary bar to the primary bar induces the large twist in its profile. Apart from a larger $\Delta\Phi$, the “arch-like” Φ profile of UGC 5903 is similar to the elliptical galaxy NGC 3226 in elliptical group 1.

The profiles of NGC 3277 and NGC 3667 appear quite similar but the strength of twist is different. Their respective twist estimated for these galaxies are $\Delta\Phi \sim 20^\circ$ and $\sim 10^\circ$. Although the profile of NGC 4714 has very small variation ($\Delta\Phi < 10^\circ$), it shows the largest scatter in this group. The overall change in the orientation of NGC 5478 is $\sim 20^\circ$. The small change ($< 10^\circ$) observed in NGC 4193 suggest that the galaxy is indeed devoid of any bar-like structure, a feature consistent with its E profile.

Group 3:

Ellipticity: The ellipticities of galaxies in this group are shown in Fig. 11. This group contains the largest number of optically classified as barred galaxies: NGC 5716, UGC 3936, NGC 4375, UGC 7073, NGC 3811, IC 742, NGC 5260, IC 1764, and UGC 3839. Qualitatively the NIR profiles of these galaxies are consistent with their optical morphology. Among these barred systems only UGC 3936 has the double-barred feature in its profile where both bars have similar strength ($E \sim 3.5$).

There are four galaxies in this group that are (optical) non-barred but have NIR features similar to optical barred systems. The galaxies are: UGC 2303, UGC 3053, IC 2947, and NGC 3618. These galaxies are labeled as “IB” in Fig. 11. Among these galaxies only one is a SA-type spiral: UGC 3053 SAcd. The UGC 2303 is likely to be a double-barred system with a secondary bar slightly stronger ($E \sim 2.5$) than the primary ($E \sim 1.5$). Apart from UGC 2303, the three other galaxies contain single bar.

The following three galaxies do not have any bar-like signature in their profiles: UGC 3296, NGC 3512, and NGC 4017. UGC 3296 is an early-type normal spiral with a profile where the ellipticity grows monotonically towards the edge. The profile of NGC 3512 indicates an oval disk where NGC 4017 is likely to have a highly flattened disk.

Note that most of the barred galaxies with distinct and strong bars(s) appear in group 2 and 3. Our measurements of ellipticities show large disagreement with 2MASS for galaxies in this group. The deviation between two estimates increases with the elongation of the disk; UGC 3839, the most flattened galaxy in this group, has the largest deviation between the two measurements.

Orientation: The orientations of galaxies are shown in Fig. 12. The overall twists ranges in between $\sim 15 - 80^\circ$. The twist as well as scatter in the orientations of these galaxies are high compared to those in previous two groups.

Among (optical) barred galaxies, UGC 3936 and UGC

3839 have the largest twist in their orientations. They both have $\Delta\Phi \sim 50^\circ$. The twist noted in the orientations of other barred galaxies are as follows: NGC 5716 : $\sim 15^\circ$, NGC 4375 : $\sim 25^\circ$, UGC 7073 : $\sim 30^\circ$, NGC 3811 : $\sim 20^\circ$, IC 742 : $\sim 15^\circ$, NGC 5260 : $\sim 20^\circ$, and IC 1764 : $\sim 15^\circ$. The Φ profile of UGC 3936 shows two different orientations likely due to its secondary and primary bar where the primary bar is highly inclined compared to the secondary.

The (optical) non-barred spirals with bar-like features in NIR (“IB”) show large twists: UGC 2303 : $\sim 60^\circ$, UGC 3053 : $\sim 30^\circ$, IC 2947 : $\sim 60^\circ$, and NGC 3618 : $\sim 30^\circ$. Two different directions of orientation is also seen in the Φ profile of UGC 2303, indicating the individual orientation of the two bars.

The orientation of NGC 3512 has $\Delta\Phi \sim 25^\circ$. UGC 3296, an intermediate-type normal spiral, show relatively smaller twist, $\sim 15^\circ$ compared to other members in this group. The largest deviation is observed in the orientation of NGC 4017. The overall twist shown by this galaxy is $\sim 80^\circ$.

Group 4:

Ellipticity: The ellipticities of galaxies in this group are shown in Fig. 13. According to RC3, the following four galaxies are barred systems: UGC 2705, UGC 3171, NGC 5510, and UGC 1478. The NIR E profiles of these galaxies have features resembling bar-like systems, in agreement with their optical morphology. The ellipticity profile of UGC 1478 shows a highly flattened central bar with a round disk.

The following eight galaxies are optically classified non-barred systems but show NIR features similar to barred galaxies: NGC 1219, NGC 6379, NGC 2416, NGC 2628, UGC 3091, UGC 7071, NGC 4584, and UGC 3233. The late-type normal spiral NGC 6379 shows a clear signature of having two distinct bars. The NIR profile of UGC 3091, a late-type transitional spiral galaxy, indicates a possible a triple-barred structure. In a previous survey of 36 spirals in B , V , R , and I wave-bands Wozniak et al. (1995) noted only three galaxies having triple bars. From our sample of 64 spirals, only 1 galaxy show a possible signature of having three bars suggesting that triple-barred disk galaxies are very rare if not uncommon. The profiles of the remaining 6 galaxies have signature of single bar.

The profiles of the following galaxies do not indicate any bar-like feature: NGC 4186, NGC 3178, NGC 4741, and UGC 1546. The ellipticity increases from the central region towards the edge. These galaxies are likely to consist of central bulge and outer disk.

Our estimate of ellipticity is consistent with 2MASS for the majority of galaxies in this group. A large disagreement is noticed for spirals with disk ellipticity $E > 3.5$ and the discrepancies arise towards the edge. Our measurement for UGC 1478 shows the largest deviation with 2MASS.

Orientation: The orientations of galaxies in spiral group 4 are shown in Fig. 14. The overall twists ranges in between $\sim 20 - 80^\circ$. The member galaxies have the highest scatter in their orientations compared to those in other three groups.

The overall twist in the orientation of the (optical) barred galaxies are, UGC 2705: $\sim 40^\circ$, UGC 3171: $\sim 20^\circ$, NGC 5510: $\sim 30^\circ$, and UGC 1478: $\sim 40^\circ$. Among the barred galaxies, the largest scatter is observed in UGC 3171. In comparison to three other galaxies above, the orientation of NGC 5510 changes gradually rather than showing any sharp

variation. UGC 1478 is the galaxy with a distinct highly flattened central bar, its orientation is constant along the central bar and changes sharply to the orientation of the disk.

The “IB” spirals have larger twists compared to their (optical) barred counterpart as mentioned above. Twists estimated for these galaxies are: NGC 1219 : $\sim 80^\circ$, NGC 6379 : $\sim 20^\circ$, NGC 2416 : $\sim 20^\circ$, NGC 2628 : $\sim 30^\circ$, UGC 3091 : $\sim 30^\circ$, UGC 7071 : $\sim 40^\circ$, NGC 4584 : $\sim 50^\circ$, and UGC 3233 : $\sim 40^\circ$. The overall change noted in the orientation of NGC 6379 is quite small compared to other spirals with double-barred feature. It suggests that both of the bars are likely to be aligned in the same direction. Apart from a large scatter, the galaxy UGC 3091 does not show any significant feature in the Φ profile to be considered as a multi-barred galaxy. The profile of NGC 4584 is atypical of a barred galaxy: constant in orientation along the bar and quickly takes another angle along the disk.

The overall twists in the orientations of the rest of the galaxies in this group are as follows: NGC 4186: $\sim 40^\circ$, NGC 3178: $\sim 60^\circ$, NGC 4741: $\sim 35^\circ$, and UGC 1546: $\sim 30^\circ$. Their Φ profiles are lack of any significant features. The nature of twist in these galaxies indicates the fact that, except NGC 4186, in the remaining three galaxies the central bulge region is less inclined compared to the outer disk.

5 CONCLUSION

We have analyzed a sample of 112 galaxies of various Hubble types obtained from 2MASS catalogue. The galaxies had been imaged in NIR J , H , and K_s bands. We have used ellipticity (E) and orientation angle (Φ) as functions of area within the isophotal contour as the diagnostic of galaxy shape constructed from a set of non-parametric shape descriptors known as the Minkowski Functionals (MFs). The ellipticity and orientation for each galaxy have been at 30 different surface brightness levels in all three bands.

Our results show that the elliptical galaxies with $E \geq 2.0$ appear to be centrally round. These galaxies show smooth variations in ellipticity with the size quantified by the area within the contour and they are more flattened near the edge. A variation as strong as $\Delta E \approx 4$ from the center towards the edge is noticeable in more flattened systems e.g. NGC 4125, NGC 3377, NGC 4008, and NGC 5791. This behavior is similar to previous studies of ellipticals in optical wavelengths (Jedrzejewski 1987, Fasano & Bonoli 1989, Franx et al. 1989). The similarity in apparent shapes in optical and NIR wavelengths indicates that the round central regions of elliptical galaxies are intrinsic rather than any artifact contributed by the seeing effect. In addition to this, the E profiles of these galaxies appear very similar in different NIR bands with a very low scatter. This evinces that the morphological differences among different bands are weak in NIR elliptical galaxies.

The twist, characterized by the change in the orientation with the size, observed in the orientations of elliptical galaxies decreases with increasing flattening. The relatively small twist noticed for ellipticals with $E > 2.0$ suggests that elongation and isophotal twist are anti-correlated in the NIR wave-bands. We performed a Spearman correlation test between the twist ($\Delta\Phi$) and the maximum ellipticity (E_{max})

obtained in our measurements. The result of test (correlation coefficient -0.31 and probability 0.091) indicates a significant anti-correlation between $\Delta\Phi$ and E_{max} (see Fig. 15). The type of correlation is similar to what has been found in the optical wavelengths by Galletta (1980). For a sample of elliptical galaxies he noticed that the maximum apparent flattening and the maximum observed twist are inversely related.

Elliptical galaxies with $E < 2.0$ usually show large variation in their orientations. These galaxies also show considerable differences both in ellipticity and orientation in different bands. The large twist observed in these ellipticals should be taken with caution since round galaxy contours are highly prone to spurious effects such as background noise.

The NIR lenticular galaxies have properties similar to that of ellipticals or disk galaxies. The E profiles of several of these galaxies show trends similar to ellipticals and few to galaxies with bar-like structures. These galaxies have, in general, large scatter in both E and Φ compared to ellipticals. In the sample of lenticular galaxies, at least 5 galaxies have bar-like signatures in their E profiles ($\sim 31\%$). The observed twists in their orientations are comparable to the trend noticed for round ($E < 2.0$) ellipticals.

The sample of spiral galaxies indicates that the bar-like feature is ubiquitous in disk galaxies without any significant dependence on Hubble's class. This sample has 64 galaxies, of which 24 are optically classified barred galaxies comprising $\sim 38\%$ of the sample. In the remaining 40 non-barred spirals, at least 21 galaxies show bar-like features in their ellipticity profiles increasing the number of bar-like systems up to $\sim 70\%$. Several previous studies have also reported higher frequency of barred systems in disk galaxies (Seiger & James 1998; Eskridge et al. 2000; Laurikainen & Salo 2002). Our result is in agreement with these studies except Seiger & James (1998) who reported $\sim 90\%$ frequency of barred galaxies from a sample of 45 spirals imaged in NIR J and K bands. Our estimate indicates that a significant fraction of disk galaxies are likely to be intrinsically non-barred systems. The absence of any bar-like structure in the E profiles of 19 spiral galaxies ($\sim 30\%$ of the sample) is in favor of this argument. This is also consistent with Eskridge et al. (2000).

Among 19 normal spirals, 17 galaxies are SA-type. The remaining two, UGC 5739 in group 1 and IC 2947 in group 3, are irregular/peculiar type galaxies. In these 17 SA-type spirals, 8 galaxies has distinct bar-like features in their shape profiles suggesting that $\sim 47\%$ of SA-type galaxies have optically hidden bars. Our result is slightly higher than Eskridge et al. (2000) who reported $\sim 40\%$ galaxies have optically hidden bars from a sample of 186 NIR H-band spirals containing 51 non-barred SA-type galaxies.

Most of the galaxies showing multiple bar features have ellipticity $E \leq 4.0$ and in more elongated galaxies this type of feature is markedly absent. The frequency of spirals with multi-barred signature is very low compared to those with single bar, only $\sim 13\%$ of the entire sample of spirals have clean signature of having two distinct bars. Our result also indicates rarity of triple-barred spiral systems, only one galaxy ($\sim 2\%$) in the entire spiral sample show this possibility. Our numbers are low compared to Wozniak et al. (1995) who reported a positive detection of double- and

triple-barred structure in 13 ($\sim 36\%$) and 3 ($\sim 9\%$) galaxies, respectively, from a sample of 36 spirals in the optical V , B , R , and I bands.

Our results indicate that in the NIR wave-bands, optically classified non-barred spirals not only show bar-like features but in a few cases they show signature of having stronger bar(s) compared to many optical barred systems. This behavior is particularly evident in NGC 3912 (group 1), UGC 5739 (group 1), NGC 4017 (group 3). Our result indicates that barred galaxies with highly flattened ($E \geq 7.0$) central bars are rare. Only two out of six spirals show central bars with $E > 7.0$. Most of barred galaxies have central ellipticity $E \geq 1$ where a few have very round centers, $E \sim 0.5$. The varying size of central round region indicates different spatial extension of central bulges within the spiral galaxies.

The shape of spiral galaxies varies a lot when the individual J , H , and K_s band measurements are compared indicating a strong color dependence for NIR spirals. The late-type normal and transitional spirals are noted to have higher scatter compared to the late-type barred spirals. In spite of different S/N ratio in these three bands, we have noticed that the measurements in J and H bands are always close compared that of K_s band for all galaxies except late-type spirals.

The overall isophotal twists observed in the orientations of spiral galaxies ranges in between $\sim 5^\circ - 80^\circ$. Many NIR barred spirals appear to have smaller but notable twists in their orientations compared to what has been noticed in the optical wavelengths (see e.g. Wozniak et al. 1995). Two conclusions can be drawn after analyzing the orientation profiles of the NIR images. First, the NIR light in J , H , and K_s bands is not fully decoupled from Population I light. They are most likely weakly coupled. Second, the different regions (central bulge, bar, and outer disk) of disk galaxies are dynamically linked. It is manifested in the steady change in the orientations of the majority of the disk galaxies. Exception is noticed in few cases, e.g. NGC 3384 (group 1), NGC 4152 (group 2), UGC2303 (group 3), where the change in the orientation is very sharp. But it is important to notice that the region where the sharp changes are observed the galaxy contours appear to very round ($E \leq 1.5$). A drastic change in the orientations of round contours do not indicate reliably the actual nature of the internal structure since these types of contours are prone to spurious effects.

Acknowledgments NR thanks to Tom Jarrett, Hume Feldman, Barbara Twarog, and Bruce Twarog for useful discussion. We acknowledge the GRF support from the University of Kansas in 2002-2003. SFS acknowledges the support from the Nonlinear Cosmology Program, 2003 at Observatory de la Cote d'Azur in Nice, France during the summer 2003 and the AAS travel grant.

This research has made use of the NASA/IPAC Infra Red Science Archive, which is operated by the Jet Propulsion Laboratory, California Institute of Technology, under contract with the National Aeronautics and Space Administration.

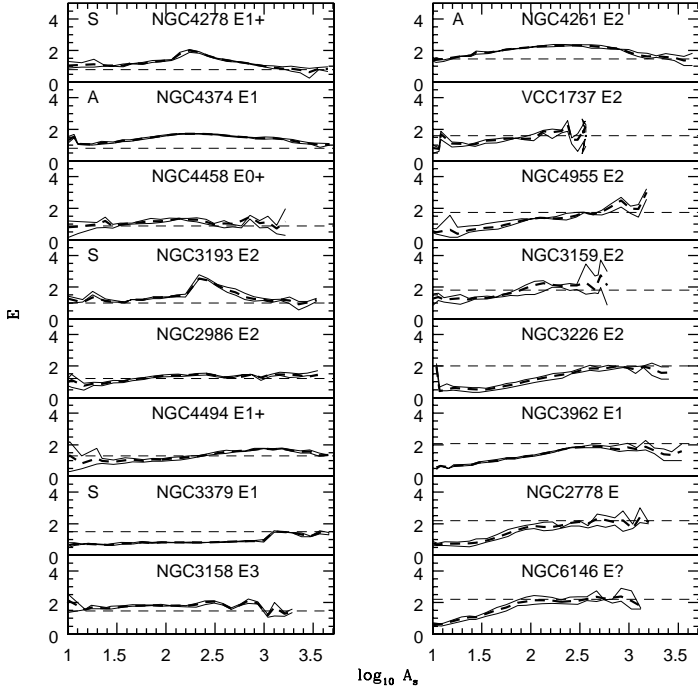


Figure 1. Ellipticity as a function of area (A_S) for elliptical galaxies in group 1 ($E \leq 2.0$). The parameter is constructed from the auxiliary ellipse of the area tensor applied to the smoothed galaxy contours. The thick dashed line represents the mean ellipticity of three different NIR bands: J , H , and K_s . The upper and lower thin solid lines are used to show the maximum and minimum ellipticity measured in these three bands. The label “A” and “S” are used to represent the respective profiles of the galaxies that appear centrally “arched” and have foreground “star” embedded into galaxy images. The horizontal dashed line represents the ellipticity of K_s band $3 - \sigma_n$ isophote measured in 2MASS. The NED galaxy name and RC3 classification are shown at the top of each panel. Note that the similar line styles are used for the rest of the presentation

6 APPENDIX

Here we briefly mention various two-dimensional Minkowski functions and also discuss the sensitivity of the Minkowski parameters.

Note that we treat every galaxy image as a set of contours where the contours are constructed by linear interpolation at different surface brightness levels. A contour is assumed to be homogeneous and have constant surface density. For a given contour i.e. at a given level, the measurement provides three scalars: A_S , P_S , and χ or Euler Characteristics (EC); three vectors (A_i , P_i , and χ_i); and a total nine components of three symmetric tensor functionals (A_{ij} , P_{ij} , and χ_{ij}). Among the scalars the A_S and P_S represent, respectively, the total area within and total perimeter along a given contour. The EC gives the number of contours at any level. For galaxy images it is always 1 irrespective of the brightness levels. The three vector functionals provide three centroids: center of mass of the area or the region within the contour (A_i), center of mass of the perimeter of the contour (P_i), and center of mass of the curvature of the contour

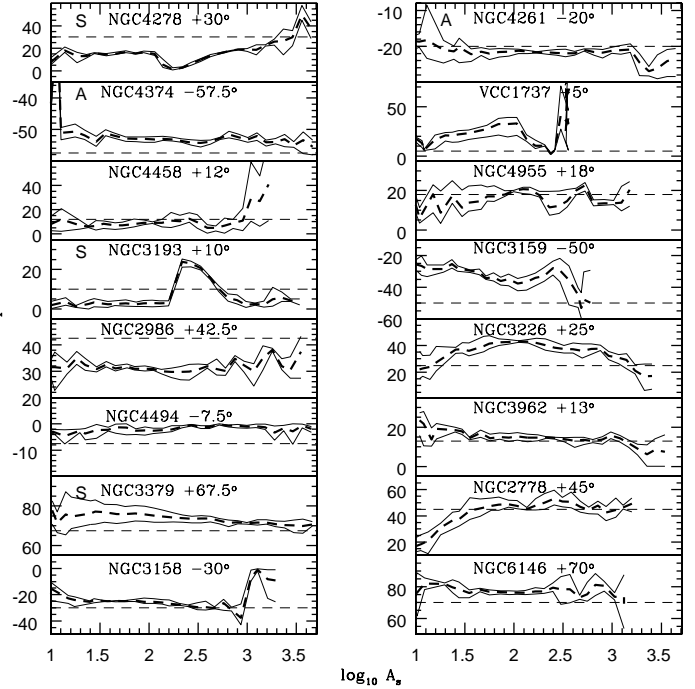


Figure 2. Orientations (in degrees) of elliptical galaxies in group 1 ($E \leq 2.0$). To present the orientations of galaxies we follow the convention where North is up and East is on the left. The label “A” and “S” are used to represent the respective profiles of the galaxies that appear centrally “arched” and have foreground “star” embedded into galaxy images. The horizontal dashed line represents the orientation of K_s band $3 - \sigma_n$ angle measured in 2MASS. The NED galaxy name and 2MASS orientation are shown at the top of each panel.

(χ). For a contour with point symmetry all three centroids will coincide irrespective of the shape. Three pair of eigen values are obtained from the components of the three tensors. Each of these pair is used to construct an ellipse that has exactly the same pair of eigen values. This is the ellipse that we call an auxiliary ellipse. Total three different auxiliary ellipses are constructed corresponding to three different tensors. Each of these ellipses is characterized by two parameters: ellipticity and orientation.

The final results presented in this study have used the parameters of the auxiliary ellipse constructed from the area tensor only since for 2MASS galaxies the perimeter and EC tensor ellipses are very similar to that of the area tensor. This is due to the highly regular appearance of NIR galaxies compared to that in the visual wavelengths. For example, a galaxy containing grand spiral arms in visual bands would lose much of its grandeur in infra red since spiral arms, mostly consist of gas and young bright stars, will be absent in that part of the spectrum. It should be mentioned here that galaxies analyzed in other wave-bands all three auxiliary ellipses will be needed for complete characterization of these objects.

In order to emphasize the features mentioned above we show the ellipticity measured from all three auxiliary ellipses both for un-smoothed and smoothed elliptical galax-

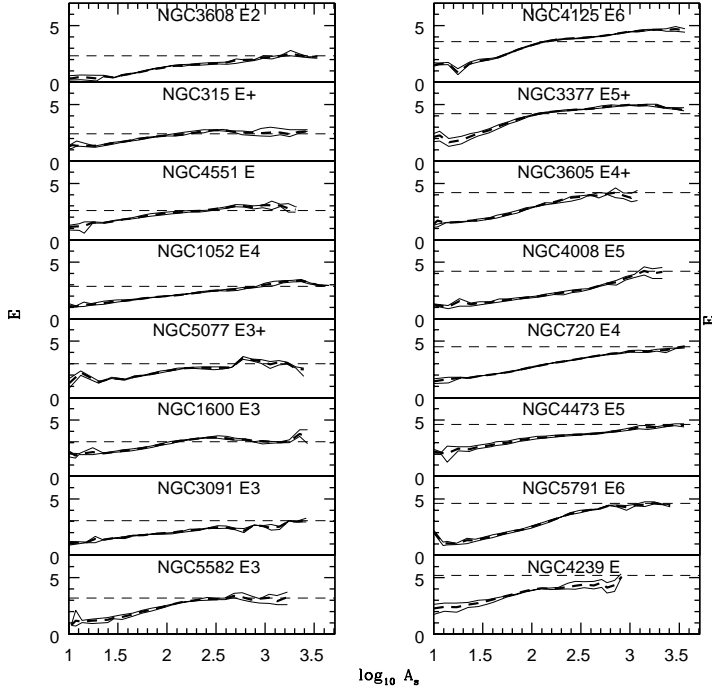


Figure 3. Ellipticity as a function of area (A_S) for elliptical galaxies in group 2 ($E > 2.0$).

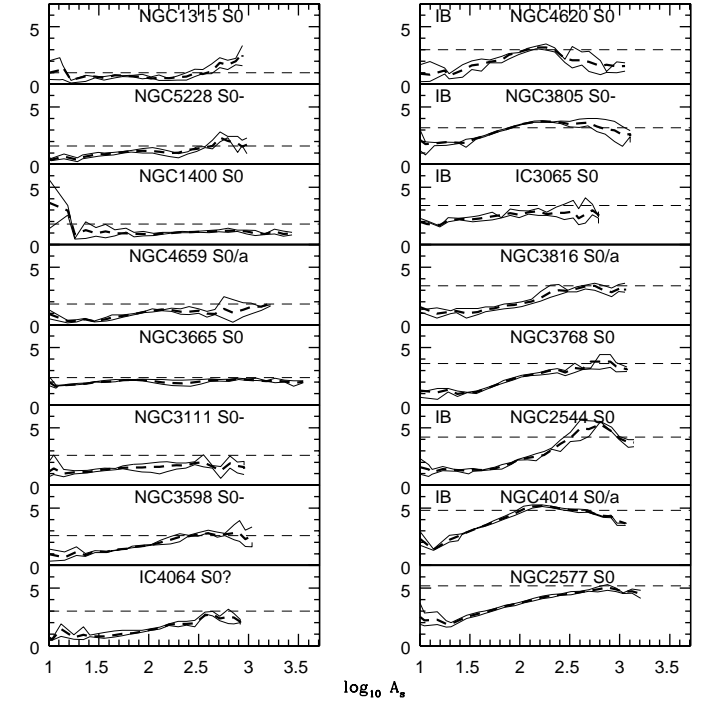


Figure 5. Ellipticity as a function of area (A_S) for lenticular galaxies. The label “IB” is used to represent the galaxy that has bar-like feature only in the infra red.

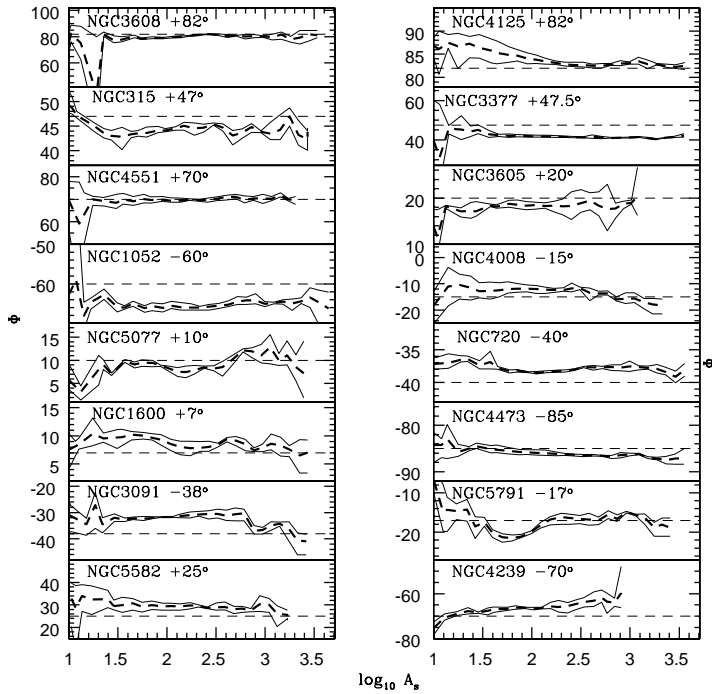


Figure 4. The orientations of elliptical galaxies in group 2 ($E > 2.0$).

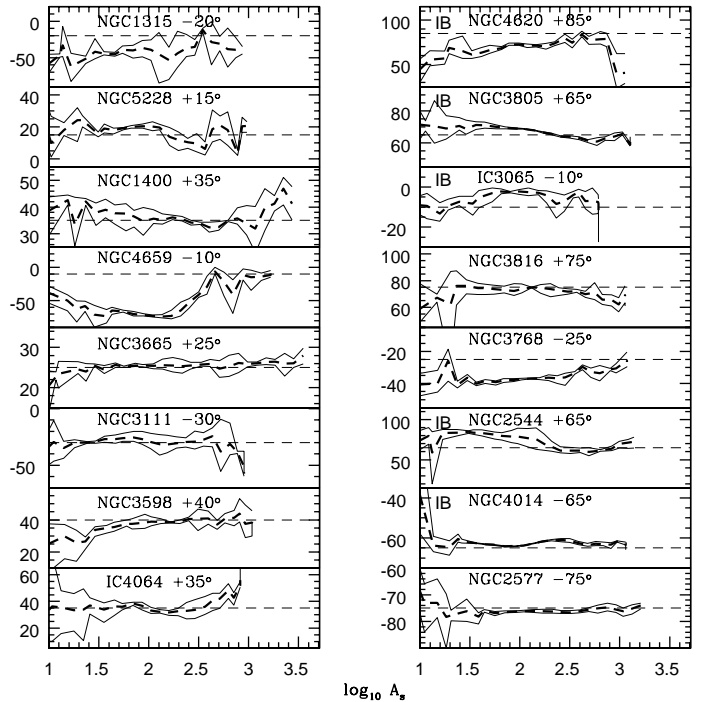


Figure 6. Orientations of lenticular galaxies shown in Fig. 5. The label “IB” is used to represent the galaxy that has bar-like feature only in the infra red.

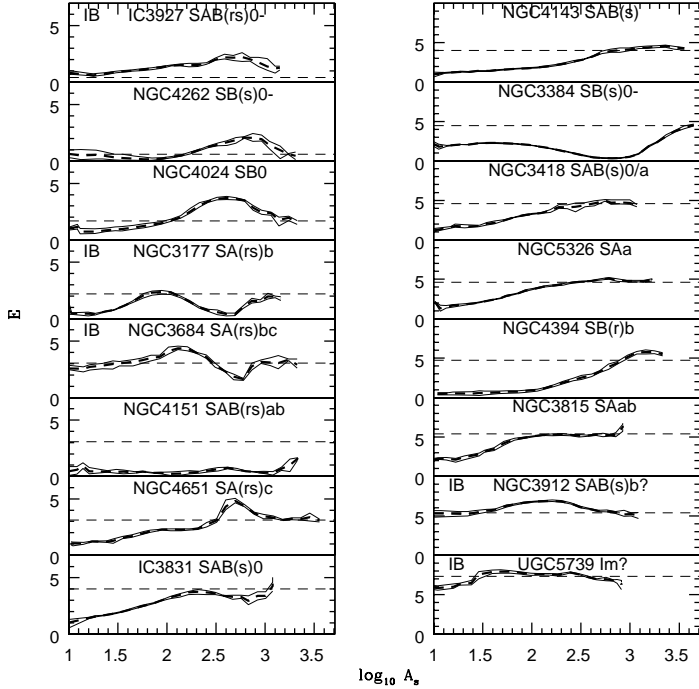


Figure 7. Ellipticity as a function of area (A_S) for spiral galaxies in group 1. The label “IB” is used to represent the galaxies that show bar-like feature only in the infra red. Note that the total spiral sample is divided into four groups. The groups are organized using the scatter (δE) observed on the ellipticity profiles in J , H , and K_s bands. Spirals in group 1 shows the least scatter ($\delta E \leq 0.5$) when ellipticity parameter is compared in three different bands whereas group 4 has the highest scatter ($\delta E \geq 2.0$). The spiral galaxies are divided into groups after visual examination.

ies in group 1. The results are presented in Fig. 16 and 17. In each of these figures the dark, medium, and light colors are used to represent the J , H , and K_s band respectively. The solid, dashed, and dashed-dotted lines show the area, perimeter, and EC ellipses for each band. As we can see for un-smoothed contours in Fig. 16, the ellipses differ from one another in each band mostly near the edge. This deviation is induced by the background noise. We should note here that a galaxy surface brightness distribution is steeper near the center and shallower outward. Due to this shallow profile any kind of background noise will have strong effect on the outer part of the distribution. Therefore when one constructs contours along the edge of a galaxy, they appear highly deviated no matter what their true shapes were. If the contours were truly elliptic, they would appear in any arbitrary shape depending on the amount distortion. Since the contours are not elliptic anymore, the auxiliary ellipses diverge from one another. This divergence reflects the apparent shape of the contours. One can see that the contour smoothing (Fig. 17) reduces the role of noise significantly and help to restore the original shape of the contours. At the same time one can also notice that the difference among the ellipses vanishes and therefore to quantify the shape of the contours using one auxiliary ellipse is as good as three ellipses.

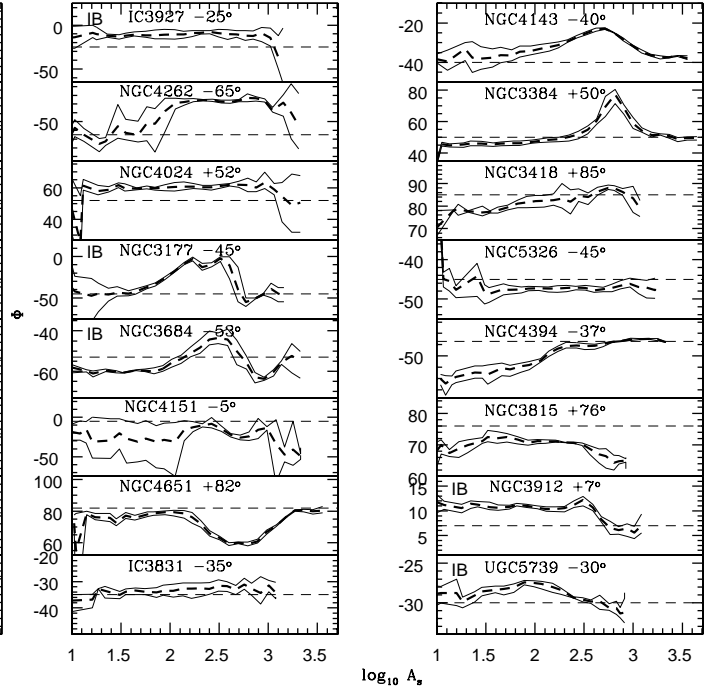


Figure 8. Orientations of galaxies in spiral group 1.

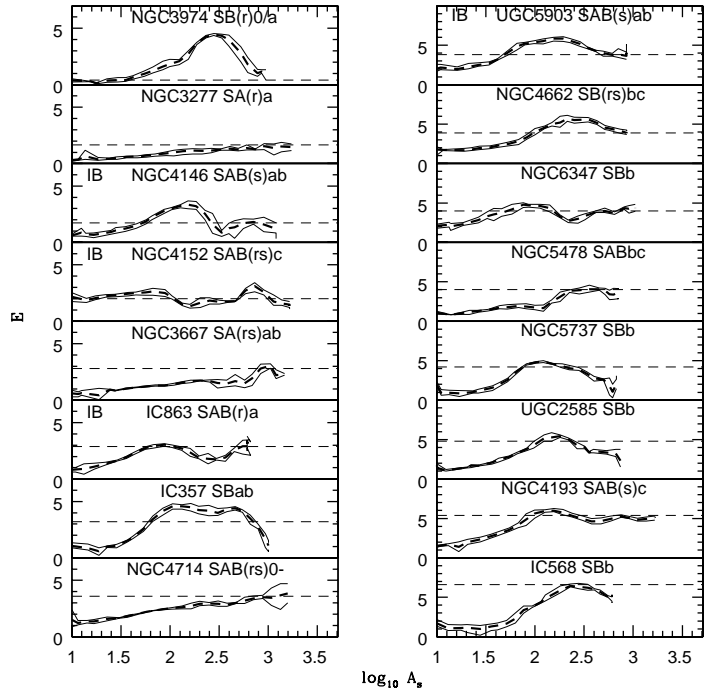


Figure 9. Ellipticity as a function of area (A_S) for spiral galaxies in group 2. The galaxies have scatter in ellipticity in the range $0.5 < \delta E \leq 1.0$ when J , H , and K_s band measurements are compared.

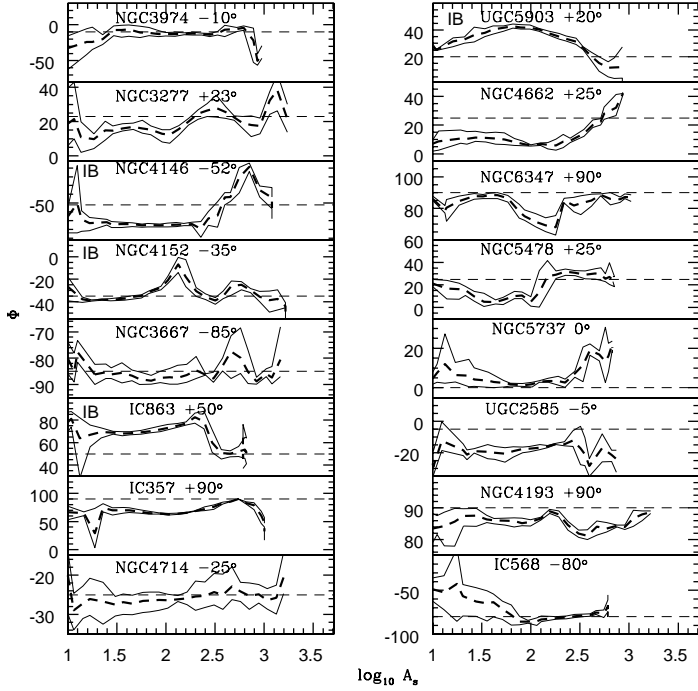


Figure 10. Orientations of galaxies in spiral group 2.

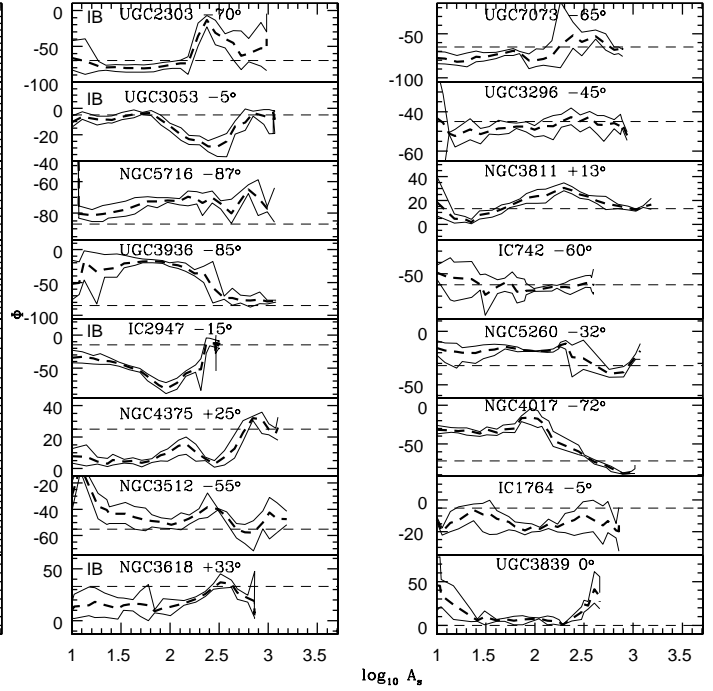


Figure 12. Orientations of galaxies in spiral group 3.

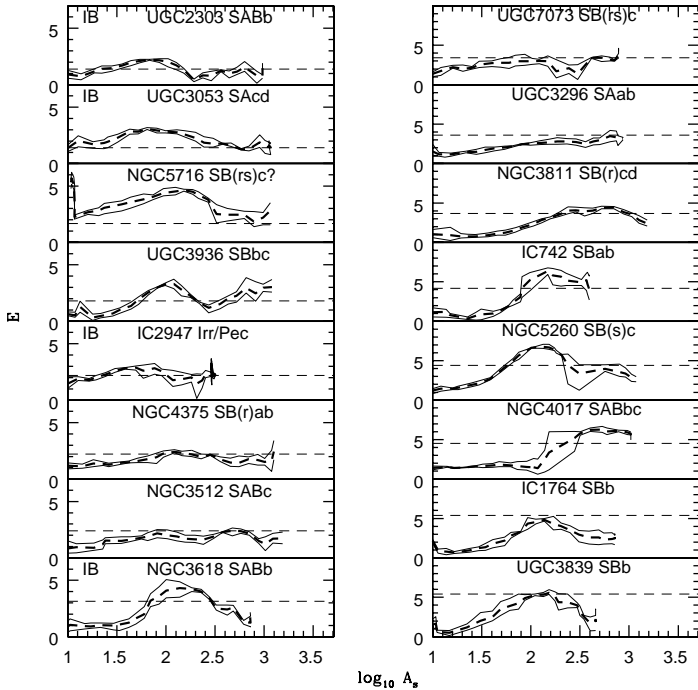


Figure 11. Ellipticity as a function of area (A_S) for spiral galaxies in group 3. The galaxies have scatter in the range, $1.0 < \delta E \leq 2.0$, in J , H , and K_s band measurements.

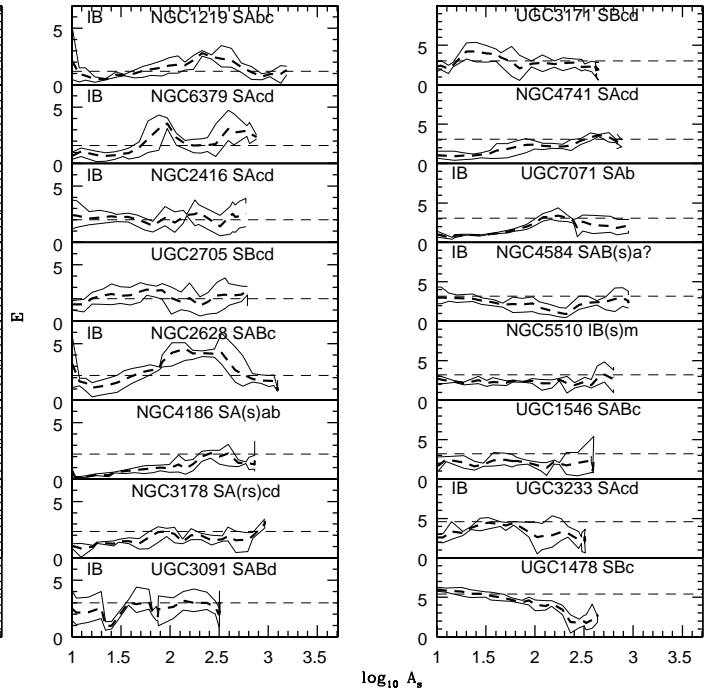


Figure 13. Ellipticity as a function of area (A_S) for spiral galaxies in group 4. The galaxies have scatter $\delta E > 2.0$ in J , H , and K_s band measurements.

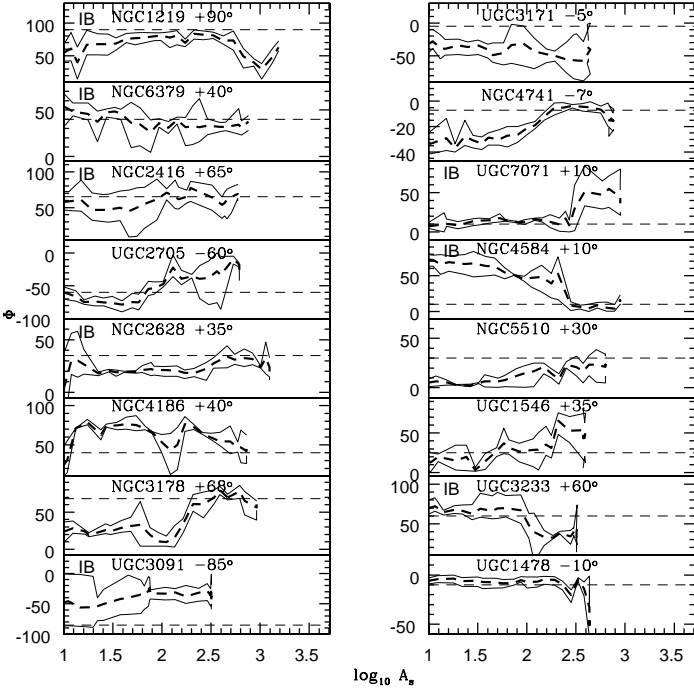


Figure 14. Orientations of galaxies in spiral group 4.

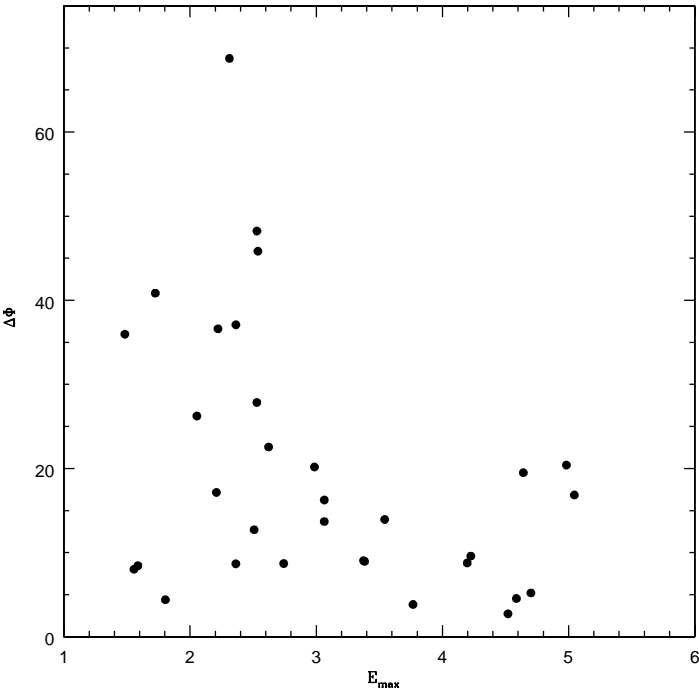


Figure 15. The twist ($\Delta\Phi$, in degrees) versus maximum ellipticity (E_{max}) plot for 32 elliptical galaxies. The result of Spearman correlation test, correlation coefficient -0.31 and the probability 0.091 , indicates a significant anti-correlation between these two parameters.

To demonstrate further, we collect first four galaxies from each group of spiral galaxies and show the E parameters for both un-smoothed and smoothed contours in Figs 18 and 19 respectively. The purpose is to re-emphasize the fact that all three auxiliary ellipses are similar and therefore the ellipse constructed from the area tensor alone is sufficient to represent even the shape of the NIR spiral galaxies.

When we compare Fig. 17 and 19, it appears that the color difference is stronger for certain types of spiral galaxies. We see that the galaxies in spiral group 4 which are mostly late-type spirals have significant differences in their shapes (at least what is revealed by the E parameter) when studied in three different NIR bands.

The galaxies with foreground stars have been included on purpose to check the sensitivity of Minkowski shape parameters as well as to emphasize the effects of foreground star(s) embedded into the galaxy image. The contours of galaxies NGC 4278, NGC 3193, and NGC 3379 are shown in Fig. 20. In this figure we also show the E measures constructed from the contours of each of these galaxies. The solid, dashed and dashed-dotted lines represent the measures from the area, perimeter and EC auxiliary ellipses as used throughout this analysis. The dotted line is the measure from the scalar functional auxiliary ellipse and has not been used in any measurement in this study. It has been included just for illustration. We should state here that the construction of scalar ellipse is different than tensor ellipses. Since the scalar functionals are simply the area (A_S) and perimeter (P_S) of a given contour, scalar ellipse is that particular ellipse which has the same area and perimeter as the contour itself. For a perfect elliptic contour the scalar auxiliary ellipse would converge with its tensor counterparts. This ellipse does not have any orientation.

As we can see a foreground star embedded into a galaxy image deviates the galaxy isophotal contours from their original shapes (usually) adding small lobe-like features to the otherwise smoothed and round contours. The functionals easily pick up this type of signal present on the contour and translate it to the shape parameters. This demonstration is to highlight the fact that the Minkowski functionals can be used for automatic detection of features attached to the image body.

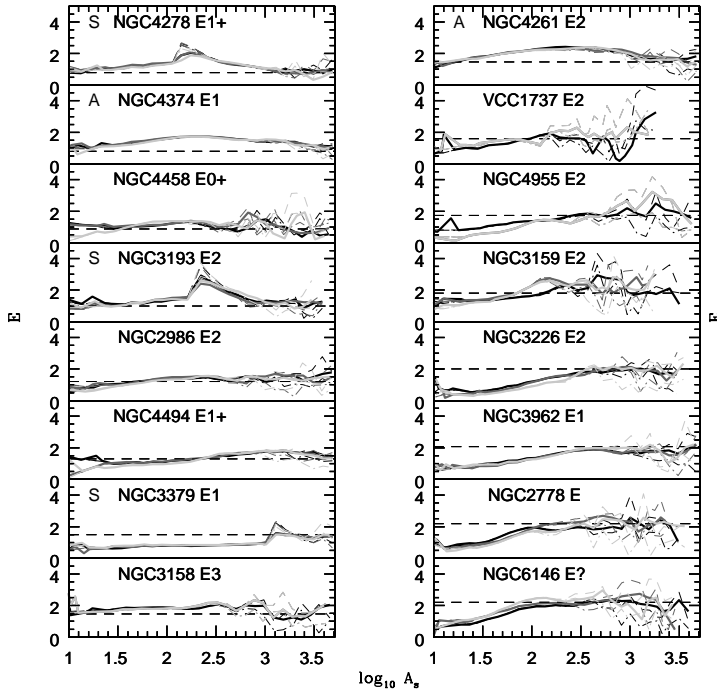


Figure 16. Ellipticity as a function of area (A_S) obtained from un-smoothed contours of elliptical galaxies in group 1. The dark, medium, and light colors are used to show the measurements from J , H , and K_s bands respectively. For each band the solid, dashed and dashed-dotted lines are used to represent the ellipticity measure of the area, perimeter and EC auxiliary ellipses. The label “A” and “S” are used to represent the respective profiles of the galaxies that appear centrally “arched” and have foreground “star” embedded into galaxy images.

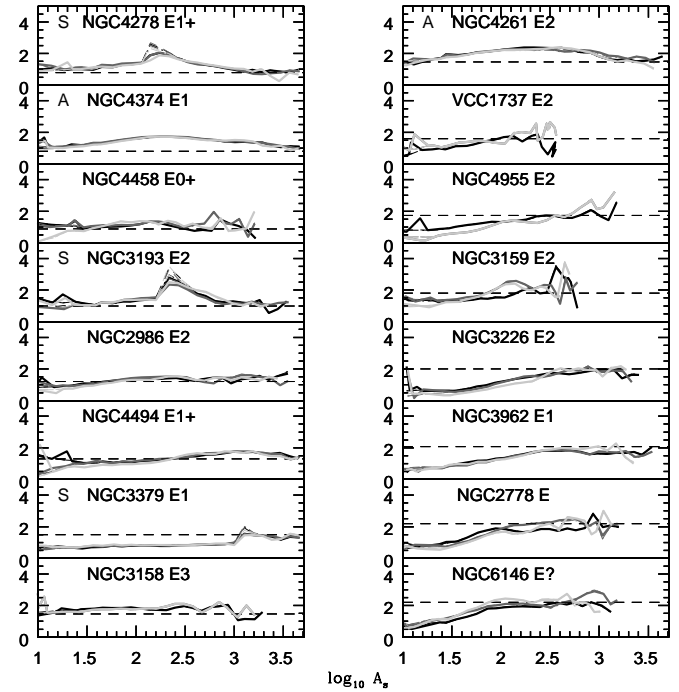


Figure 17. Ellipticity as a function of area (A_S) for smoothed contours of elliptical galaxies in group 1. The line styles and colors are similar to Fig. 16. Notice how contour smoothing reduces the effect of noise retaining the main features of the contours. The solid, dashed, and dashed-dotted lines representing different auxiliary ellipses for each band converge and stay on top of one other. The convergence indicates that the galaxy contours are indeed elliptical in nature which is revealed as a result of smoothing.

REFERENCES

- Abraham R. G., Merrifield M. R., Ellis R. S., Tanvir N. R., Brinchmann J., 1999, *MNRAS*, 308, 569
- Abraham R. G., Merrifield M. R., 2000, *ApJ*, 120, 2835
- Athanassoula E., Morin S., Wozniak H., Puy D., Pierce M. J., Lombard J., Bosma A., 1990, *MNRAS*, 245, 130
- Bender R., Möllenhoff C., 1987, *A&A*, 177, 71
- Beisbart C., 2000, Ph.D. Thesis, Ludwig-Maximilians-Universität, München, Germany
- Beisbart C., Buchert T., Wagner H., 2001a, *Physica A*, 293, 592B
- Beisbart C., Valdarnini R., Buchert T., 2001b, *A&A*, 379, 412
- Carter D., 1978, *MNRAS*, 182, 797
- de Vaucouleurs G., de Vaucouleurs A., Corwin H. G. Jr., Buta R., Paturel G., Fouqué P., 1991, *Third Reference Catalogue of Bright Galaxies* (Berlin: Springer) (RC3)
- Eskridge P. B. et al., 2000, *AJ*, 119, 536
- Fasano G., Bonoli C., 1989, *A&ASS*, 79, 291
- Franx M., Illingworth G., Heckman T., 1989, *AJ*, 98, 538
- Galletta G., 1980, *A&A*, 81, 179
- Hobson M. P., Jones A. W., Lasenby A. N., 1999, *MNRAS*, 309, 125
- Jarrett T. H., 2000, *PASP*, 112, 1008
- Jarrett T. H., Chester T., Cutri R., Schneider S., Skrutskie R., Huchra J. P., 2000, *ApJ*, 119, 2498
- Jarrett T. H., Chester T., Cutri R., Schneider S., Skrutskie R., Huchra J. P., 2003, *AJ*, 125, 525
- Jedrzejewski R. I., 1987, in *Structure and Dynamics of Elliptical Galaxies*, ed. T. de Zeeuw, (Dordrecht: Reidel), p. 37
- Kerscher M. et al., 1997, *MNRAS*, 284, 73
- Kerscher M., Mecke K., Schmalzing J., Beisbart C., Buchert T., Wagner H., 2001a, *A&A*, 373, 1
- Kerscher M. et al., 2001b, *A&A*, 377, 1
- Leach R., 1981, *ApJ*, 248, 485
- Lauer T., 1985, *MNRAS*, 216, 429
- Laurikainen E., Salo H., Rautiainen P., 2002, *MNRAS*, 331, 880
- Laurikainen E., Salo H., 2002, *MNRAS*, 337, 1118
- Martin P., 1995, *AJ*, 109, 2428
- Mecke K. R., Buchert T., Wagner H., 1994, *A&A*, 288, 697
- Minkowski H., 1903, *Math. Ann.*, 57, 447
- Novikov D., Feldman H. A., Shandarin S. F., 1999, *Int. J. Mod. Phys.*, D8, 291
- Novikov D., Schmalzing J., Mukhanov V. F., 2000, *A&A*, 364, 17
- Peletier, R. F., Davis, R. L., Illingworth, G. D., Davis, L. E., Cawson M., 1990, *AJ*, 100, 1091
- Rahman N., Shandarin S. F., 2003, *MNRAS*, 343, 933
- Rozas M., Knapen J. H., Beckman J. E., 1998, *MNRAS*, 301, 631
- Schmalzing J., Buchert T., 1997, *ApJ*, 482, L1
- Schmalzing J., Gorski K. M., 1998, *MNRAS*, 297, 355
- Schmalzing J., Buchert T., Melott A. L., Sahni V., Sathyaprakash B. S., Shandarin S. F., *ApJ*, 526, 568
- Seigar M. S., James P. A., 1998, *MNRAS*, 299, 672
- Shandarin S. F., 2002, *MNRAS*, 331, 865
- Shandarin S. F., Feldman H. A., Xu Y., Tegmark M., 2002, *ApJS*, 141, 1
- Sheth J., Sahni V., Shandarin S. F., Sathyaprakash B. S., 2003,

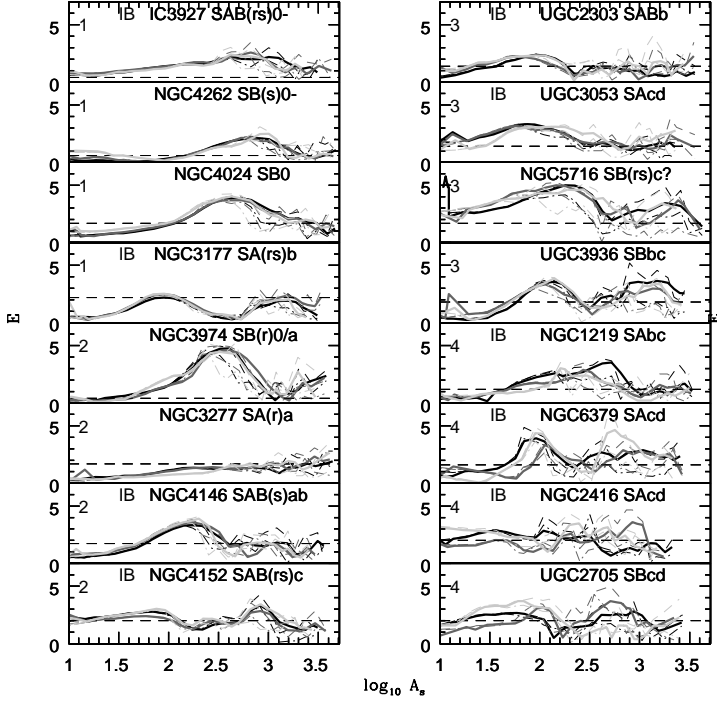


Figure 18. Ellipticity as a function of area (A_S) obtained from un-smoothed contours of spiral galaxies. The first four galaxies from each spiral group are shown in this figure marked by numbers 1 to 4 where 1 stands for group 1 and so on. The line styles and colors are similar to Fig. 16.

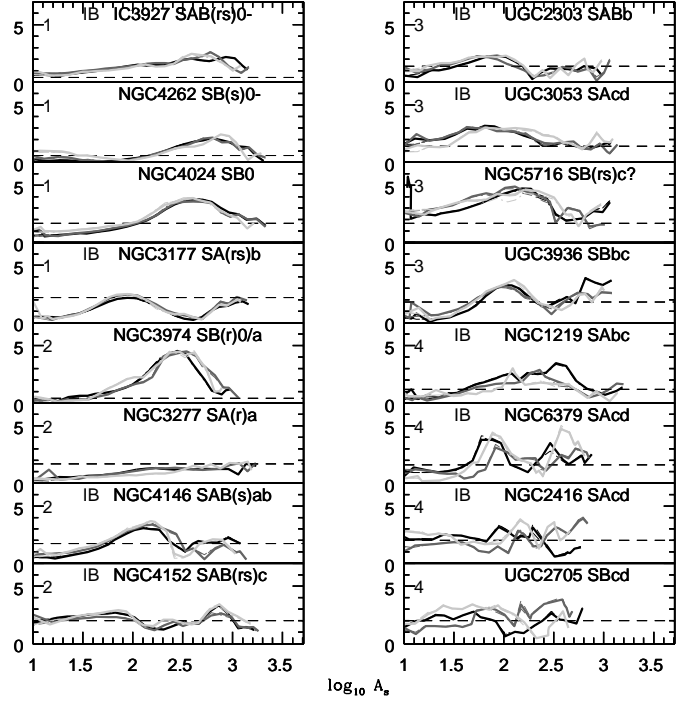


Figure 19. Ellipticity as a function of area (A_S) for smoothed contours of spiral galaxies in Fig. 18. The line styles and colors are similar as before. The convergence of the auxiliary ellipses as a result of smoothing illustrates the fact that the contours of the spiral galaxies are elliptic in nature although the ellipticity varies with image size. In comparison to Fig. 18, one can see that contour smoothing reduces noise keeping the main features intact. One can also notice that the color difference is stronger in late type spirals (lower four panels on the right, marked with the number 4).

MNRAS, 343, 22S

Williams T. B., Schwarzschild M., 1979, ApJ, 227, 56

Wozniak H., Pierce M. J., 1991, A&AS, 88, 325

Wozniak H., Friedli D., Martinet L., Martin P., Bratschi P., 1995, A&ASS, 111, 115

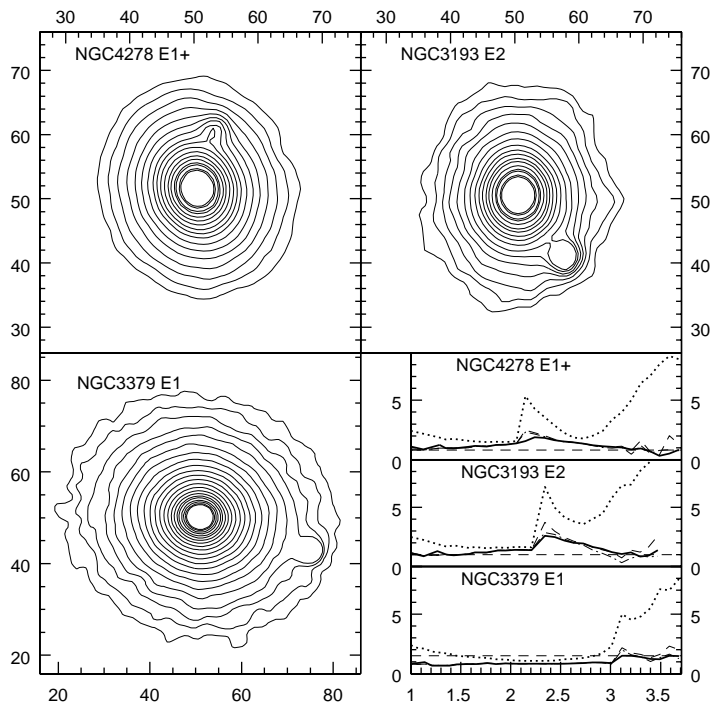


Figure 20. The un-smoothed contour plot of galaxies where the foreground star is embedded in galaxy images and the behavior of E parameters constructed from different MFs. The dotted line represents ellipticity from the scalar functional (not used in the present analysis); the (thick) solid, dashed, and dashed-dotted line represent ellipticity of the auxiliary ellipses constructed from the area, perimeter, and EC tensor respectively. The presence of lobe-like feature and sharp kink in the ellipticity parameter give the signature of embedded foreground star(s).